

# Matter Effects in Atmospheric Neutrino Oscillations

E. Akhmedov<sup>1</sup>, P. Lipari and M. Lusignoli

*Dipartimento di Fisica, Università di Roma "la Sapienza",  
and I.N.F.N., Sezione di Roma,  
Piazzale A. Moro 2, I-00185 Roma, Italy*

## Abstract

The Kamiokande II and IMB data on contained events induced by atmospheric neutrinos exhibit too low a ratio of muons to electrons, which has been interpreted as a possible indication of neutrino oscillations. At the same time, the recent data on upward-going muons in underground detectors have shown no evidence for neutrino oscillations, strongly limiting the allowed region of oscillation parameter space. In this paper we confront different types of neutrino oscillation hypotheses with the experimental results. The matter effects in  $\nu_\mu \leftrightarrow \nu_e$  and in  $\nu_\mu \leftrightarrow \nu_{sterile}$  oscillations are discussed and shown to affect significantly the upward-going muons.

Several times signals of neutrino oscillations have been claimed in the past. The evidence from accelerator and reactor experiments has meanwhile evaporated [1], leaving the observed solar neutrino deficit as the only possible indication.

Recently, however, another hint of neutrino oscillations has been obtained. The Kamiokande II [2] and IMB [3] collaborations observed an anomaly in the contained neutrino induced events. Both groups measure the ratio of muons to electrons and find it smaller than what is predicted by several independent theoretical calculations [4]. The events observed in these experiments have charged lepton energies in the range from a few hundred MeV to 1.2 GeV. A possible interpretation of the effect has been given in terms of  $\nu_\mu \leftrightarrow \nu_x$  oscillations, where  $\nu_x$  can be  $\nu_e$ ,  $\nu_\tau$  or a sterile neutrino ( $\nu_s$ ), with typical values for the oscillation parameters  $\Delta m^2 \sim 10^{-3} \div 10^{-2} \text{ eV}^2$  and  $\sin^2 2\theta \geq 0.5$  (a summary is contained in ref. [5]). For this range of parameters, the flux of upward-going muons could also be observably reduced. However, the IMB and Baksan experiments did not observe any such reduction [6, 7], thus setting rather stringent limits to the allowed region in the  $(\Delta m^2, \sin^2 2\theta)$  plane.

Neutrino oscillations (in vacuum [8] or in solar matter [9]) are also the most popular explanation for the solar neutrino deficit. In this case the  $\nu_e$  must oscillate into a neutrino of different flavour. However, both problems cannot be solved through the same  $\nu_e \leftrightarrow \nu_\mu$  oscillations, since the ranges of  $\Delta m^2$  required in the two cases do not overlap. Thus, if the solar neutrino problem is solved through  $\nu_e \leftrightarrow \nu_\mu$  oscillations, then the atmospheric  $\nu_\mu$ 's must oscillate into something else. The simplest and often made hypothesis is that the contained events anomaly is explained through the  $\nu_\mu \leftrightarrow \nu_\tau$  oscillations. In this case, since both neutrino flavours have identical interactions with matter, the oscillations will

---

<sup>1</sup>On leave from Kurchatov Institute of Atomic Energy, Moscow 123182, Russia

not be affected by the presence of the matter in the earth. If, however, the initial  $\nu_\mu$  oscillates to  $\nu_e$  or to a sterile neutrino,  $\nu_s$ , the matter effects can be relevant.

In this letter we shall discuss in detail the various scenarios for atmospheric neutrino oscillations and show that indeed the matter effects are important, in that the allowed parameter region for both  $\nu_\mu \leftrightarrow \nu_e$  and  $\nu_\mu \leftrightarrow \nu_s$  oscillations is appreciably different as compared to the  $\nu_\mu \leftrightarrow \nu_\tau$  case.

The evolution equation [9] of a system of two neutrino species  $(\nu_i, \nu_j)$  in matter is

$$i \frac{d}{dt} \begin{pmatrix} \nu_i \\ \nu_j \end{pmatrix} = \frac{\Delta m^2}{4E} \begin{pmatrix} 2v_i(t) - \cos 2\theta & \sin 2\theta \\ \sin 2\theta & 2v_j(t) + \cos 2\theta \end{pmatrix} \begin{pmatrix} \nu_i \\ \nu_j \end{pmatrix} \quad (1)$$

Here  $i, j = e, \mu, \tau$  or  $s$  where  $\nu_s$  is a sterile neutrino,  $i \neq j$ ,  $\theta$  is the  $\nu_i$ — $\nu_j$  mixing angle in vacuum ( $0 \leq \theta \leq \pi/4$ ),  $\Delta m^2 = m_2^2 - m_1^2$ , where we assume  $\nu_i$  to be a predominant component of the mass eigenstate  $\nu_1$ , and

$$v_e(t) = \frac{2\sqrt{2}EG_F}{\Delta m^2} \left[ N_e(t) - \frac{N_n(t)}{2} \right], \quad (2)$$

$$v_\mu(t) = v_\tau(t) = \frac{2\sqrt{2}EG_F}{\Delta m^2} \left[ -\frac{N_n(t)}{2} \right], \quad (3)$$

$$v_s(t) = 0 \quad (4)$$

where  $N_e$  and  $N_n$  are the electron and neutron number densities and  $G_F$  is the Fermi constant. The evolution of the antineutrino system is described by the same equation with  $v_{i,j}(t)$  substituted by  $-v_{i,j}(t)$ .

In matter of constant density the probability of  $\nu_i \leftrightarrow \nu_j$  oscillations has the same form as in vacuum with the amplitude  $\sin^2 2\theta$  and oscillation length  $\ell = 4\pi E/\Delta m^2$  substituted by

$$\sin^2 2\theta_m = \frac{\sin^2 2\theta}{[(v_i - v_j) - \cos 2\theta]^2 + \sin^2 2\theta}, \quad (5)$$

$$\ell_m = \frac{\ell}{\{[(v_i - v_j) - \cos 2\theta]^2 + \sin^2 2\theta\}^{1/2}} \quad (6)$$

It can be seen from eq.(5) that matter can either enhance or suppress oscillations depending on the relative signs and magnitudes of  $(v_i - v_j)$ , and  $\cos 2\theta$ . Note that  $(v_i - v_j)$  changes its sign with  $\Delta m^2$ . If the condition

$$v_i - v_j = \cos 2\theta \quad (7)$$

is satisfied, the amplitude of oscillations in matter  $\sin^2 2\theta_m$  becomes equal to unity, and the oscillations are resonantly enhanced (the MSW effect). The probability of the  $\nu_i \rightarrow \nu_j$  transition will be large provided matter density varies slowly enough along the neutrino trajectory, i.e. the adiabaticity condition is fulfilled. In matter with uniform (or nearly uniform) density the transition probability will crucially depend on the thickness of the

matter slab. In general one needs to integrate numerically the evolution equation (1) along the neutrino path.

The effect of matter on  $\sin^2 2\theta_m$  in the case of  $\nu_\mu \leftrightarrow \nu_e$  oscillations is illustrated in fig. 1, where it is plotted as a function of  $\Delta m^2/E$ , assuming a density  $\rho = 5 \text{ g cm}^{-3}$ , and an electron fraction  $N_e/(N_p + N_n) = 1/2$  (this corresponds to approximately average values in the earth). We can distinguish three regions: if  $\Delta m^2/E \gtrsim 10^{-2} \text{ eV}^2/\text{GeV}$ , the matter effects are negligible; if  $\Delta m^2/E \lesssim 10^{-4} \text{ eV}^2/\text{GeV}$ , the matter effect suppresses strongly the oscillation probabilities, and mixing in matter almost vanishes; in the transition region for  $\Delta m^2 > 0$  ( $\Delta m^2 < 0$ ) the neutrino (antineutrino) mixing parameter passes through a resonance  $\sin^2(2\theta_m) = 1$  of width proportional to  $\tan 2\theta$ , while the antineutrino (neutrino) effective mixing parameter goes to zero monotonically as the energy increases. In the case of maximal mixing in vacuum the oscillation probabilities of neutrinos and antineutrinos are equal and the sign of  $\Delta m^2$  is irrelevant.

The case of  $\nu_\mu \leftrightarrow \nu_s$  oscillations can be calculated as before with the substitution  $N_e(t) \rightarrow -N_n(t)/2$ . The change of sign has the consequence that now for  $\Delta m^2 > 0$  ( $\Delta m^2 < 0$ ) it is the antineutrino (neutrino) that will pass through the resonance. Since in the earth  $N_n \simeq N_p = N_e$ , fig. 1 can also be interpreted as describing the dependence on  $\Delta m^2/E$  of the mixing parameter  $\sin^2(2\theta_m)$  in the case of  $\nu_\mu \leftrightarrow \nu_s$  oscillations in matter with a density of  $10 \text{ g cm}^{-3}$ , interchanging the neutrino and antineutrino curves.

Atmospheric neutrinos are produced in the hadronic shower induced by primary cosmic rays in the earth's atmosphere. These neutrinos can be observed directly in large mass underground detectors by means of their charged-current interactions. "Contained events" are those where the neutrino-nucleus interaction vertex is located inside the detector and all final state particles do not get out from it. The average energy of the neutrinos that give rise to these events is a few hundred MeV.

Muon neutrinos can also be detected indirectly observing the muons that they have produced in the material surrounding the detector. To reduce the background from atmospheric muons, only upward-going neutrino-induced muons are usually considered. A rough estimate of the energy spectrum of the upward-going muons has been obtained dividing them in two categories, passing (those of highest energy) and stopping muons.

The flux of upward-going muons can be calculated as

$$\phi_{\mu^\mp}(E_\mu, \cos \psi) = \int_{E_\mu}^{\infty} dE_\nu \phi_{\nu_\mu(\bar{\nu}_\mu)}(E_\nu, \cos \psi) \frac{dn_{\nu_\mu(\bar{\nu}_\mu) \rightarrow \mu^\mp}(E_\mu; E_\nu)}{dE_\mu} \quad (8)$$

where  $\phi_{\nu_\mu(\bar{\nu}_\mu)}(E_\nu, \cos \psi)$  is the  $\nu_\mu$  ( $\bar{\nu}_\mu$ ) spectrum at nadir angle  $\psi$ , and  $dn_{\nu_\mu(\bar{\nu}_\mu) \rightarrow \mu^\mp}/dE_\mu$  is the number of  $\mu^\mp$  with energy between  $E_\mu$  and  $E_\mu + dE_\mu$  produced by a neutrino (antineutrino) of energy  $E_\nu$ :

$$\frac{dn_{\nu_\mu(\bar{\nu}_\mu) \rightarrow \mu^\mp}(E_\mu; E_\nu)}{dE_\mu} = N_A \int_0^\infty dX \int_{E_\mu}^{E_\nu} dE_0 \frac{d\sigma_{\nu_\mu(\bar{\nu}_\mu)}(E_0, E_\nu)}{dE_0} \delta[E_\mu - R^{-1}(R(E_0) - X)] \quad (9)$$

In this equation, the first integral is over the position of neutrino absorption ( $X$  is in  $\text{g cm}^{-2}$ ,  $X = 0$  corresponds to the detector); the second integral is over the muon energy at the production point. The delta function expresses the fact that the muon created with initial energy  $E_0$  at the point  $X$  must reach the detector with energy  $E_\mu$ . In the argument of the delta function,  $R(E)$  is the range in rock of a muon of energy  $E$ , and  $R^{-1}(X)$  is the inverse function, giving the initial energy of a muon with range  $X$ . We are assuming that fluctuations in the energy loss are negligible, and that the energy-range relation is well defined. This is a good approximation in this range of muon energy (see ref. [10] for a discussion). The neutrino cross section, expressed in terms of the usual kinematical variables  $y = 1 - E_\mu/E_\nu$ , and  $x = Q^2/(2m_N E_\nu y)$ , can be calculated integrating over  $x$  the following expression:

$$\frac{d^2\sigma_\nu}{dx dy}(x, y, E_\nu) = \frac{2G_F^2 m_N E_\nu}{\pi} \left[ \frac{M_W^2}{M_W^2 + Q^2} \right]^2 x [q_d(x, Q^2) + (1-y)^2 \bar{q}_u(x, Q^2)] \quad (10)$$

In eq. (10)  $G_F$  is the Fermi constant,  $M_W$  is the  $W$  boson mass,  $m_N$  is the nucleon mass, and  $q_{d,u}$  ( $\bar{q}_{d,u}$ ) are the distributions of quarks (antiquarks) of down-like and up-like type in the target nucleon. The antineutrino cross section is obtained interchanging  $q \leftrightarrow \bar{q}$ .

Eq. (8) assumes that the neutrino flux is unmodified in the passage through the earth. To take into account the effects of oscillations we have to make the substitution

$$\phi_{\nu_\mu} \rightarrow [1 - P_{\nu_\mu \rightarrow \nu_x}] \phi_{\nu_\mu} \quad (11)$$

for  $\nu_x = \nu_\tau$  or  $\nu_s$ , or

$$\phi_{\nu_\mu} \rightarrow [1 - P_{\nu_\mu \rightarrow \nu_e}] \phi_{\nu_\mu} + P_{\nu_e \rightarrow \nu_\mu} \phi_{\nu_e} \quad (12)$$

in the case of  $\nu_\mu \leftrightarrow \nu_e$  oscillations, and analogously for antineutrinos.

Strictly speaking, the transition probability  $P_{\nu_\mu \rightarrow \nu_x}$  depends on the oscillation parameters  $\Delta m^2$  and  $\sin^2 2\theta$ , neutrino energy  $E_\nu$ , nadir angle  $\psi$ , and also on the exact positions of creation and absorption points of neutrinos. The neutrinos are produced in a layer of the atmosphere with a thickness of approximately  $\sim 10$  km, and the upward-going muons are created in a layer of thickness  $\sim 0.1$  km below the detector. We will be discussing a range of  $\Delta m^2/E$  such that  $\ell > 100$  km and therefore it is a good approximation to neglect the dependence on the exact position of creation and absorption of the neutrinos, and assume that all neutrinos are generated in an infinitely thin spherical layer of atmosphere at the surface of the earth and that the muons are also produced in a thin layer of material below the detector. In this approximation the  $\nu_\mu \leftrightarrow \nu_\tau$  transition probability takes the form:

$$P_{\nu_\mu \leftrightarrow \nu_\tau} \left( \frac{E}{\Delta m^2}, \cos \psi \right) = \frac{1}{2} \sin^2 2\theta \left[ 1 - \cos \left( \frac{\Delta m^2 R_\oplus \cos \psi}{E} \right) \right]. \quad (13)$$

The probability of  $\bar{\nu}_\mu \leftrightarrow \bar{\nu}_\tau$  transition is equal to that in the neutrino case.

The probabilities of the neutrino (and antineutrino) transitions  $\nu_\mu \leftrightarrow \nu_e$  and  $\nu_\mu \leftrightarrow \nu_s$  have been calculated by integrating numerically the evolution equation (1) using the distributions of  $N_e(r)$  and  $N_n(r)$  obtained from the matter density profile of the earth

taken from ref. [11] and assuming  $N_n \simeq N_p = N_e$ , which is quite a good approximation in the interior of the earth.

Some effects of neutrino oscillations on the upward-going muon flux are described below. (i) The total rate is reduced with respect to expectations based on the assumption of no oscillations. To detect this effect one needs to control the absolute normalization of the calculated flux. (ii) The energy spectrum is distorted, because low energy neutrinos have a shorter oscillation length. The shape of the neutrino spectrum, after the crossing of the earth, is reflected in the energy spectrum of the upward-going muons. The ratio of stopping/passing muons in an underground detector is therefore a useful tool in the search for neutrino oscillations. In this measurement one needs only to control the shape (and not the normalization) of the calculated upward-going muon flux. A large part of the uncertainties in the calculations cancel, and the measurement is thus dominated by statistical errors. (iii) The nadir angle distribution is also modified, because longer path lengths correspond to more vertical directions.

In our numerical work we have defined as “stopping muons” those with energy ( $1.25 \text{ GeV} \leq E_\mu \leq 2.5 \text{ GeV}$ ), and “passing muons” those with ( $E_\mu \geq 2.5 \text{ GeV}$ ). Integrating over the entire downward hemisphere the muon flux given in eq. (8) we obtain the integrated fluxes

$$\Phi_{s(p)}^\pm = 2\pi \int_0^1 d\cos\psi \int_{1.25(2.5)}^{2.5(\infty)} dE_\mu \phi_{\mu^\pm}(E_\mu, \cos\psi). \quad (14)$$

In general the oscillation probabilities of neutrinos and antineutrinos are different, and therefore we compute separately the fluxes of positive and negative muons. However the existing detectors are unable to measure the charge of the detected particles, and so we then add together the calculated  $\mu^\pm$  fluxes. The total flux of upward-going muons is  $\Phi = \Phi_s + \Phi_p = \Phi_s^+ + \Phi_s^- + \Phi_p^+ + \Phi_p^-$ .

In the calculation of the upward-going muon fluxes in the absence of oscillations, one needs to specify the neutrino fluxes, the nucleon structure functions (needed in the calculation of the cross section), and the muon range. The imperfect knowledge of the first and second item introduce a significant systematic uncertainty. Using the  $(\nu_\mu + \bar{\nu}_\mu)$  flux calculated by Volkova [12], with the  $\nu/\bar{\nu}$  ratio of Lipari [13], the structure functions given by Diemoz *et al.* [14], and the muon range taken from the report of Lohmann *et al.* [15], the calculated flux of upward-going muons is:

$$\frac{\Phi_s + \Phi_p}{2\pi} = 2.36 \cdot 10^{-13} (\text{cm}^2 \text{ s sr})^{-1} \quad (15)$$

(0.70 of the flux is due to negative muons), and

$$\frac{\Phi_s}{\Phi_p} = 0.185 \quad (16)$$

(0.67 of the stopping muons are negative). The median energy of neutrinos giving rise to stopping (passing) muons is 5.5 (86) GeV. A different choice of the input in equation (8)

would modify these results, in particular there is a large sensitivity to the neutrino fluxes. Using the neutrino fluxes of Butkevich *et al.* [16], results in a total upward-going muon flux larger than (15) by 11%. In this case the stopping/passing ratio is 0.189, a difference of less than 3%. Using the  $(\nu_\mu + \bar{\nu}_\mu)$  fluxes of Mitsui [17] would result in a total flux 6% (5.5%) larger than (15) and a ratio of stopping to passing of 0.191 (0.190), with the  $\nu/\bar{\nu}$  ratio of Butkevich (Lipari). The calculations with the structure functions of Eichten *et al.* [18] result in a rate of muons smaller by 1% for set 1, and larger by 2.5% for set 2.

The calculated upward-going muon flux (14) is implicitly a function of the oscillation parameters. Given the flavour of the neutrino mixed with the  $\nu_\mu$ , each choice of a pair of parameters  $(\Delta m^2, \sin^2 2\theta)$  will result in a different flux. As an illustration, in fig. 2 we show the calculated  $\Phi_s/\Phi_p$  ratio as a function of  $\Delta m^2$  assuming maximal mixing ( $\sin^2 2\theta = 1$ ). It is clear that the matter effect is important and that the curves corresponding to  $\nu_\tau$ ,  $\nu_e$  and  $\nu_s$  differ from each other. The qualitative behaviour of the curves can be simply understood. For  $\Delta m^2 < 10^{-4} \text{ eV}^2$ , the oscillation length even of the softest neutrinos that produce detectable muons is longer than the earth's radius, and there is no visible effect. With increasing  $\Delta m^2$  the low energy neutrinos begin to oscillate, the spectrum is distorted and  $\Phi_s/\Phi_p$  decreases. For  $\Delta m^2 > 1 \text{ eV}^2$ , all relevant neutrino energies are equally affected and, averaging over the very rapid oscillations, the shape of the spectrum is again the same as in the no-oscillation case. In the case of  $\nu_\mu \leftrightarrow \nu_e$  oscillations we have to consider the presence of the  $\nu_e(\bar{\nu}_e)$  directly produced in meson decay. These neutrinos have a much steeper spectrum than the  $\nu_\mu(\bar{\nu}_\mu)$ . For large  $\Delta m^2$  averaging over rapid undetectable oscillations we have:  $\phi_{\nu_\mu} \rightarrow (1 - 0.5 \sin^2 2\theta)\phi_{\nu_\mu} + 0.5 \sin^2 2\theta \phi_{\nu_e}$ . This yields a distortion of the spectrum with a relative excess of low energy neutrinos.

Measured values of the upward-going muon flux (averaged over  $2\pi$  of solid angle), in units  $10^{-13} (\text{cm}^2 \text{ s sr})^{-1}$ , are:  $(2.77 \pm 0.17)$  with a threshold of 1 GeV from the Baksan group [7],  $(2.26 \pm 0.17)$  with a threshold of 2 GeV from the IMB experiment [19],  $(2.04 \pm 0.13)$  with a threshold of approximately 3 GeV from the Kamiokande experiment [20]. The three measurements, after corrections for the different thresholds, are in agreement with each other, and very close to our calculated value (15). To obtain an allowed region in the  $(\Delta m^2, \sin^2 2\theta)$  plane would require a detailed discussion of the systematic uncertainties of the theoretical calculation. The IMB group [6] derives a rather stringent limit from their measurement of the total rate of upward-going muons. A more critical view of the systematic uncertainties, however, would result in much less stringent limit [21]. Rather arbitrarily, we have chosen as a criterion to define the region of parameter space that can be excluded at 90% c.l. because of the measurement of the total rate the condition

$$\Phi \leq 0.75 \Phi_0, \quad (17)$$

$\Phi_0$  being the average flux (15) calculated in the absence of oscillations. The limiting curves calculated using this criterion (curves of type A) for different types of oscillations are shown in fig. 3 for the  $\nu_\mu \leftrightarrow \nu_\tau$  and  $\nu_\mu \leftrightarrow \nu_s$  cases, and in fig. 4 for the  $\nu_\mu \leftrightarrow \nu_e$  case.

The IMB collaboration has measured [6] a stopping/passing ratio  $0.160 \pm 0.019$ , in

good agreement with their detailed Monte Carlo predictions. Our calculated value of 0.185 agrees reasonably well with the IMB result, considering the approximations we have used<sup>2</sup>. In this case we have used as a criterion (90% c.l.) for oscillations the condition:

$$\frac{\Phi_s}{\Phi_p} \leq 0.8 \left( \frac{\Phi_s}{\Phi_p} \right)_0 \quad (18)$$

where again the subscript indicates the ratio of fluxes calculated in the absence of neutrino oscillations. Curves calculated with this criterion (curves of type *B*) are shown in fig. 3 for the  $\nu_\mu \leftrightarrow \nu_\tau$  and  $\nu_\mu \leftrightarrow \nu_s$  cases. For the  $\nu_\mu \leftrightarrow \nu_e$  oscillations the condition (18) is never satisfied. In fig. 4 we show the region of parameter space that could be excluded with the requirement  $\Phi_s/\Phi_p \leq 0.9 (\Phi_s/\Phi_p)_0$ , more demanding from the point of view of statistical accuracy.

The situation about experimentally allowed values of oscillation parameters in the case of  $\nu_\mu \leftrightarrow \nu_\tau$  and  $\nu_\mu \leftrightarrow \nu_s$  oscillations is summarized in fig. 3. In this figure three limiting curves are the results of experiments that do *not* involve upward-going muons. Curve (a) is obtained from accelerator experiments [22] and the allowed region is below the curve. Curve (b) is obtained from the result of Fréjus [23] on the  $e/\mu$  ratio of contained events; this result is consistent with the no-oscillation hypothesis, and the allowed region is to the left of the curve. Curve (c) is obtained from the observation of an anomaly in the same  $e/\mu$  ratio by Kamiokande and IMB [2, 3]; this is a ‘positive result’ and the allowed region is to the right of the curve. These three limits apply equally to  $\nu_\mu \leftrightarrow \nu_\tau$  and  $\nu_\mu \leftrightarrow \nu_s$  oscillations which differ from each other only because of the matter effects. These effects are obviously irrelevant to the accelerator limit, and almost so also for (b) and (c) curves, although approximately half of the contained events observed in IMB and Kamiokande are produced by neutrinos that have penetrated through the earth. In fact, these neutrinos have energies  $E_\nu \leq 1.2$  GeV, with a rapidly falling spectrum. On curves (b) and (c) the absolute value of the squared mass difference is always larger than  $10^{-3}$  eV<sup>2</sup>. For matter effects to be significant one needs

$$\frac{\Delta m^2}{E} \lesssim \sqrt{2} G_F N_A \rho = 0.758 \cdot 10^{-4} \rho (\text{g cm}^{-3}) \frac{\text{eV}^2}{\text{GeV}} \quad (19)$$

The maximum density of the earth is  $\rho \simeq 12.5$  g cm<sup>-3</sup>, therefore for contained events matter effects are practically negligible and their inclusion would only slightly modify the shape of curve (c) in the region of lowest  $|\Delta m^2|$ .

Matter effects are on the contrary significant for upward-going muons, the reason being that the neutrino energies involved are one to two orders of magnitude larger than those for contained events.

---

<sup>2</sup>In the IMB detector the threshold energy for muon detection was approximately 1.8 GeV in the initial part of the data taking (IMB-1,2), and 1.0 GeV for the final part (IMB-3). The criterion for stopping muons is that there is essentially no light for the last 5 meters of the projected track length inside the detector. Considering the geometrical dimension of the detector ( $18 \times 17 \times 22.5$  m<sup>3</sup>), this sets a maximum energy for stopping muon of  $\sim 2.5$  GeV.

The limits obtained from the total flux of upward-going muons using the criterion (17) are shown in fig. 3 by the curves  $A_\tau$ ,  $A_{s+}$  and  $A_{s-}$ , the subscript indicating the flavour of the neutrino mixed with the  $\nu_\tau$ . The case  $\nu_s$  is described by two curves because we need to consider the sign of  $\Delta m^2$ . The limits obtained from the stopping/passing ratio using the criterion (18) are shown in the same figure by the curves  $B_\tau$ ,  $B_{s+}$  and  $B_{s-}$ .

Comparing the three type A curves we can make the following remarks. For maximal mixing the limits on  $|\Delta m^2|$  for  $\nu_\mu \leftrightarrow \nu_s$  oscillations is a factor 2.6 less stringent than for  $\nu_\mu \leftrightarrow \nu_\tau$ . If  $\sin^2 2\theta = 1$  the matter can only suppress the oscillations, in fact  $\nu_\mu$ 's with  $|\Delta m^2|/E \lesssim 2 \cdot 10^{-4} \text{ eV}^2/\text{GeV}$  have their mixing with  $\nu_s$  strongly suppressed (see fig. 1) and do not oscillate. For maximal mixing the sign of  $\Delta m^2$  is irrelevant and therefore the curves  $A_{s+}$  and  $A_{s-}$  end at the same point. With decreasing mixing the two curves separate, the limit for negative  $\Delta m^2$  being stronger. When  $\Delta m^2 < 0$  ( $\Delta m^2 > 0$ ) for oscillations of neutrinos (antineutrinos) the MSW resonant enhancement will occur. Since  $\nu_\mu$ 's are more abundant (and have a larger cross section) than  $\bar{\nu}_\mu$ 's, the same values of  $\sin^2 2\theta$  and  $|\Delta m^2|$  will result in a stronger suppression of the upward-going muon flux if  $\Delta m^2$  is negative and the MSW resonance is relevant for neutrinos. For  $|\Delta m^2| \gtrsim 1 \text{ eV}^2$  the three curves  $A_\tau$ ,  $A_{s+}$  and  $A_{s-}$  almost coincide; this is again a reflection of the fact that for large  $|\Delta m^2|/E$  matter effects are not significant.

Very similar considerations can be made about the curves  $B_\tau$ ,  $B_{s+}$  and  $B_{s-}$ . For maximal mixing, the region of  $|\Delta m^2|$  that can be excluded in the case of  $\nu_\mu \leftrightarrow \nu_s$  oscillations is moved to values of  $|\Delta m^2|$  larger by a factor 2.8 than in the  $\nu_\mu \leftrightarrow \nu_\tau$  case. For oscillations into sterile neutrinos, when the mixing is smaller than unity, the limit that applies for  $\Delta m^2 < 0$  is stronger than for the other case. This is again because when the MSW resonance occurs for neutrinos (antineutrinos) the sensitivity to oscillations is stronger (weaker). A detailed analysis must also take into account the fact that when the neutrinos resonate the oscillation length passes through a maximum. This is the reason why the limit  $B_{s+}$  is stronger than the limit  $B_{s-}$  in a limited region of parameter space. For maximal mixing the curves  $B_{s+}$  and  $B_{s-}$  end in the same points.

The most significant difference between the limits for  $\nu_\mu \leftrightarrow \nu_\tau$  and  $\nu_\mu \leftrightarrow \nu_s$  oscillations is in the region of low squared mass differences. A region of parameter space  $|\Delta m^2| = (3 \div 7) \cdot 10^{-4} \text{ eV}^2$  and  $\sin^2 2\theta \geq 0.7$  is excluded for  $\nu_\tau$  but not for  $\nu_s$  oscillations. This region is however already excluded by curve (c), provided that the anomaly in the  $e/\mu$  ratio of contained events is due to neutrino oscillations. As shown in fig. 3, for both types of oscillations there is a region of parameter space which is compatible with all existing experimental measurements. The range of allowed values for the parameters is in both cases roughly:  $0.4 \lesssim \sin^2 2\theta \lesssim 0.7$  and  $2 \cdot 10^{-3} \text{ (eV}^2) \lesssim |\Delta m^2| \lesssim 0.4 \text{ (eV}^2)$ . The allowed region for  $\nu_s$  is somewhat smaller but contains also a small part (for large positive  $\Delta m^2$ ) which is not allowed for  $\nu_\tau$ . In future, with more data, the sensitivity of the curves of type B (which is determined by the statistical errors) will improve, exploring the low  $|\Delta m^2|$  part of the allowed region. To improve the sensitivity of the curves of type A, one needs rather to reduce the theoretical systematic uncertainties. If these could be reduced to the level of 15% (at 90% c.l.) the entire allowed region of parameter space would then be explored by measurements of upward-going muons and one would be able to either



confirm or disprove the neutrino oscillations as a solution to the atmospheric neutrino puzzle.

The situation about the experimentally allowed values of the oscillation parameters in the case of  $\nu_\mu \leftrightarrow \nu_e$  oscillations is summarized in fig. 4. The results from the analysis of solar neutrino experiments refer to lower values of  $|\Delta m^2|$  and are not shown. As in fig. 3, three limiting curves are the results of experiments that do *not* involve upward-going muons. Curve (a) is the limit obtained from reactor experiments [24], curve (b) and (c) are obtained from measurements of the  $e/\mu$  ratio of contained events in the Fréjus [23] and Kamiokande and IMB experiments [2, 3]. As before, curve (b) excludes the region to its right, curve (c) the region to its left.

The limits obtained from the measurement of the total upward-going muon flux according to criterion (17) is shown by curves  $A_{e+}$  and  $A_{e-}$ , the two curves referring to the sign of  $\Delta m^2$  as before. The region excluded by the curves of type  $A$  is well inside the region of parameter space already excluded by the Gösgen reactor experiment. Matter suppresses the oscillations more strongly than in the  $\nu_\mu \leftrightarrow \nu_s$  case, since the difference in the effective potentials is twice as large now, see eqs. (2,3,4). We also have to take into account the fact that in cosmic ray showers a  $\nu_e(\bar{\nu}_e)$  flux is produced as well. Both effects reduce the sensitivity of the measurement to  $\nu_\mu \leftrightarrow \nu_e$  oscillations.

As already mentioned, the condition (18) is never satisfied, and therefore no limit can be obtained from the stopping/passing ratio. In the case of maximal mixing,  $\Phi_s/\Phi_p$  reaches (for  $|\Delta m^2| = 6 \cdot 10^{-2} \text{eV}^2$ ) a minimum value of 0.150, only 19% smaller than the value calculated in the absence of oscillations. Curves  $B_{e+}$  and  $B_{e-}$  are calculated with the more demanding criterion  $\Phi_s/\Phi_p \leq 0.9 (\Phi_s/\Phi_p)_0$ . They are an indication of the sensitivity that could be obtained with a sample of data approximately four times the one collected by IMB.

As shown in fig. 4, a small region of parameter space  $0.35 \lesssim \sin^2 2\theta \lesssim 0.7$  and  $4 \cdot 10^{-3} (\text{eV}^2) \lesssim |\Delta m^2| \lesssim 2 \cdot 10^{-2} (\text{eV}^2)$  is compatible with all existing experimental measurements. Future experiments on upward muon fluxes will be able to explore only a part of this region.

As we have seen, the oscillations of  $\nu_\mu$  into a sterile neutrino state  $\nu_s$  can be strongly affected by the matter of the earth. Although the existence of a sterile neutrino does not contradict any laboratory data, it can be in conflict with cosmological considerations. Namely, for large enough values of the mixing angle and  $\Delta m^2$ ,  $\nu_\mu \leftrightarrow \nu_s$  oscillations can bring the sterile neutrinos into equilibrium with matter before the nucleosynthesis epoch [25] thereby affecting the primordial  ${}^4\text{He}$  abundance in the universe. The analysis performed in [26] sets the maximum allowed number of “light neutrinos”  $N_\nu$  to 3.4. The limit derived in [27] not to have  $N_\nu > 3.4$  for oscillations between sterile and muon neutrinos is  $\Delta m^2 < 8 \cdot 10^{-6} \text{eV}^2$  for maximal mixing. With the values we obtained in our analysis this bound would be violated, and we would have  $N_\nu = 4$ . The limit given in [26] is not however universally accepted and is still a point of debate [28], so that we believe that  $\nu_\mu \leftrightarrow \nu_s$  oscillations may still provide a viable solution to the atmospheric neutrino

problem.

As to the  $\nu_\mu \leftrightarrow \nu_e$  oscillations hypothesis for atmospheric neutrinos, it should be noted that this assumption does not contradict the idea of neutrino oscillations being also responsible for the observed solar neutrino deficit. The latter can be accounted for through the  $\nu_e \leftrightarrow \nu_\tau$  oscillations provided the neutrino masses obey the conditions  $m_{\nu_e} \approx m_{\nu_\tau} \ll m_{\nu_\mu}$  or  $m_{\nu_\mu} \ll m_{\nu_e} \approx m_{\nu_\tau}$ . We would like to stress that although many models (including those implementing the see-saw mechanism [29] of neutrino mass generation) predict the neutrino mass hierarchy  $m_{\nu_e} \ll m_{\nu_\mu} \ll m_{\nu_\tau}$ , models with quite different hierarchies also exist. Moreover, there are absolutely no experimental indications in favour of the direct hierarchy.

In summary, we have shown that the complex of data induced by atmospheric neutrinos (“contained” and “upward-going muons”) may still be described in terms of neutrino oscillations. The matter effects are important in the precise determination of the allowed parameter region.

P.L. is grateful to T.K. Gaisser and T. Stanev for many useful conversations and for showing us an early version of ref. [21]. E.A. acknowledges fruitful discussions with Z. Berezhiani and A. Smirnov.

## Figure Captions

Fig. 1. Plot of  $\sin^2 2\theta_m$ , the mixing parameter in matter for  $\nu_\mu \leftrightarrow \nu_e$  oscillations, as a function of  $\Delta m^2/E$ , for  $\sin^2 2\theta = 1, 0.5, 0.05$ , assuming a matter density  $\rho = 5 \text{ g cm}^{-3}$  and an electron fraction  $Y_e = 0.5$ . Solid curves are for neutrinos, dashed curves for antineutrinos. If  $\Delta m^2 < 0$  the neutrino and antineutrino curves must be interchanged. The same curves can also be interpreted as the mixing parameter in matter for the  $\nu_\mu \leftrightarrow \nu_s$  transition, assuming a matter density  $\rho' = 10 \text{ g cm}^{-3}$  and interchanging the neutrino and antineutrino curves.

Fig. 2. Plot of the  $\Phi_s/\Phi_p$  ratio as a function of  $|\Delta m^2|$ , assuming maximal mixing in vacuum. The different curves are for  $\nu_\mu \leftrightarrow \nu_\tau$ ,  $\nu_\mu \leftrightarrow \nu_e$ , and  $\nu_\mu \leftrightarrow \nu_s$  oscillations. We also show the curve calculated for the  $\nu_\mu \leftrightarrow \nu_e$  transitions neglecting the  $\nu_e(\bar{\nu}_e)$  created directly in meson decays.

Fig. 3. Limits for the oscillation parameters  $\Delta m^2$  and  $\sin^2 2\theta$  in the case of  $\nu_\mu \leftrightarrow \nu_\tau$  and  $\nu_\mu \leftrightarrow \nu_s$  mixing. The curves  $A_\tau$ ,  $A_{s+}$  and  $A_{s-}$  are limits obtained from the measurements of the total flux of upward-going muons. The curves  $B_\tau$ ,  $B_{s+}$  and  $B_{s-}$  are obtained from the measurements of the stopping/passing ratio. Also plotted are the 90% c.l. limits from accelerator experiments (a), and the from the measurement of the  $e/\mu$  ratio of contained events in the Fréjus (b) and Kamiokande experiments (c).

Fig. 4. Limits for the oscillation parameters  $\Delta m^2$  and  $\sin^2 2\theta$  in the case of  $\nu_\mu \leftrightarrow \nu_e$  mixing. The curves  $A_{e+}$  and  $A_{e-}$  are obtained from the measurements of the total flux of upward-going muons. The curves  $B_{e+}$  and  $B_{e-}$  are in this case estimates of the sensitivity of future measurements of the stopping/passing ratio (see text). Also plotted are the 90% c.l. limits from the Gösgen reactor experiment (a), and from the  $e/\mu$  ratio of contained events in Fréjus (b), and Kamiokande (c).

## References

- [1] R. Maschuw, Proceedings of Joint International Lepton-Photon Symposium and EPS Conference on High Energy Physics, Geneva, Switzerland, july-august 1991, Vol. I, page 619.
- [2] K.S. Hirata *et al.* (Kam-II Collaboration), Physics Letters B 280 (1992) 146.
- [3] R. Becker-Szendy *et al.* (IMB Collaboration), Phys. Rev. D 46, (1992) 3720. See also D. Casper *et al.*, Phys. Rev. Lett. 66 (1991) 2561.
- [4] G. Barr, T.K. Gaisser & Todor Stanev, Phys. Rev. D39 (1989) 3532; H. Lee & Y.S. Koh, Nuovo Cimento B 105 (1990) 883; M. Honda, K. Kasahara, K. Hidaka & S. Midorikawa, Phys. Lett. B248 (1990) 193; M. Kawasaki & S. Mizuta, Phys. Rev. D43 (1991) 2900; E.V. Bugaev & V.A. Naumov, Phys. Lett. B 232 (1989) 391.
- [5] E.W. Beier *et al.*, Phys. Lett. B 283 (1992) 446.
- [6] R. Becker-Szendy *et al.* (IMB Collaboration), Phys. Rev. Lett. 69 (1992) 1010.
- [7] M.M. Boliev *et al.* (Baksan Collaboration), in Proc. 3rd Int. Workshop on Neutrino Telescopes (ed. Milla Baldo Ceolin) (1991), 235.
- [8] B. Pontecorvo, Zh. Eksp. Teor. Fiz. 34 (1958) 247.
- [9] S.P. Mikheyev, A.Yu. Smirnov, Yad. Fiz. 42, 1441 (1985) [Sov. J. Nucl. Phys. 42, 913 (1985)]; L. Wolfenstein, Phys. Rev. D 17, 2369 (1978).
- [10] Paolo Lipari & Todor Stanev, Phys. Rev. D44 (1991) 3543.
- [11] F.D. Stacey, "Physics of the earth" Wiley, New York, 1969, p. 281.
- [12] L.V. Volkova, Yad. Fiz. 31 (1980) 784 (Sov. J. Nucl. Phys. 31 (1980) 1510).
- [13] P. Lipari, Astroparticle Physics, to be published.
- [14] M. Diemoz, F. Ferroni, E. Longo & G. Martinelli, Z.Phys. C 39 (1988) 21.
- [15] W. Lohmann, R. Kopp & R. Voss, CERN Yellow Report No. EP/85-03.
- [16] A.V. Butkevich, L.G. Dedenko & I.M. Zheleznykh, Yad. Fiz. 50 (1989) 142 (Sov. J. Nucl. Phys. 50 (1989) 90).
- [17] K. Mitsui, Y. Minorikawa & H. Komori, Nuovo Cimento 9C (1986) 995.
- [18] E. Eichten, I. Hinchcliffe, K. Lane & C. Quigg, Rev. Mod. Phys. 56 (1984) 579 (Erratum 58 (1986) 1065).
- [19] R. Becker-Szendy *et al.*, Singapore High Energy Physics Conference, p.662, (1990).

- [20] M. Mori *et al.* (Kamiokande collaboration), Phys. Lett. B 270 (1991) 89.
- [21] W. Frati, T.K. Gaisser, A.K. Mann, Todor Stanev, submitted to Phys. Rev. D and private communication.
- [22] F. Dydak *et al.* (CDHS collaboration), Phys. Lett. B 134 (1984) 281; F. Bergsma *et al.* (CHARM collaboration), Phys. Lett. B 142 (1984) 183.
- [23] Ch. Berger *et al.* (Fréjus collaboration), Phys. Lett. B 245 (1990) 305; B 227 (1989) 489.
- [24] G. Zacek *et al.*, Phys. Rev. D 34 (1986) 2621.
- [25] A.D. Dolgov, Yad. Fiz. 33 (1981) 1309 [Sov. J. Nucl. Phys. 33, (1981) 700]; M.Yu. Khlopov, S.T. Petcov, Phys. Lett. B 99 (1981) 117; B 100 (1981) 520 (E); A.D. Dolgov, D.P. Kirillova, Intern. J. Mod. Phys. A 3 (1988) 267; R. Barbieri, A. Dolgov, Phys. Lett. B 237 (1990) 440; Nucl. Phys. B349 (1991) 743; K. Kainulainen, Phys. Lett. B 244 (1990) 191.
- [26] K.A. Olive, D.N. Schramm, G. Steigman, T.P. Walker, Phys. Lett. B 236 (1990) 454.
- [27] K. Enqvist, K. Kainulainen, M. Thomson, Phys. Rev. Lett. 68 (1992) 744; Nucl. Phys. B 373 (1992) 498.
- [28] A. Hime, R.J.N. Phillips, G.G. Ross, S. Sarkar, Phys. Lett. B 260 (1991) 381.
- [29] M. Gell–Mann, P. Ramond, R. Slansky, in Supergravity, edited by D. Freedman *et al.*, North-Holland, Amsterdam, 1979; T. Yanagida, KEK Lectures, 1979 (unpublished); R.N. Mohapatra, G. Senjanović, Phys. Rev. Lett. 44 (1980) 912 .

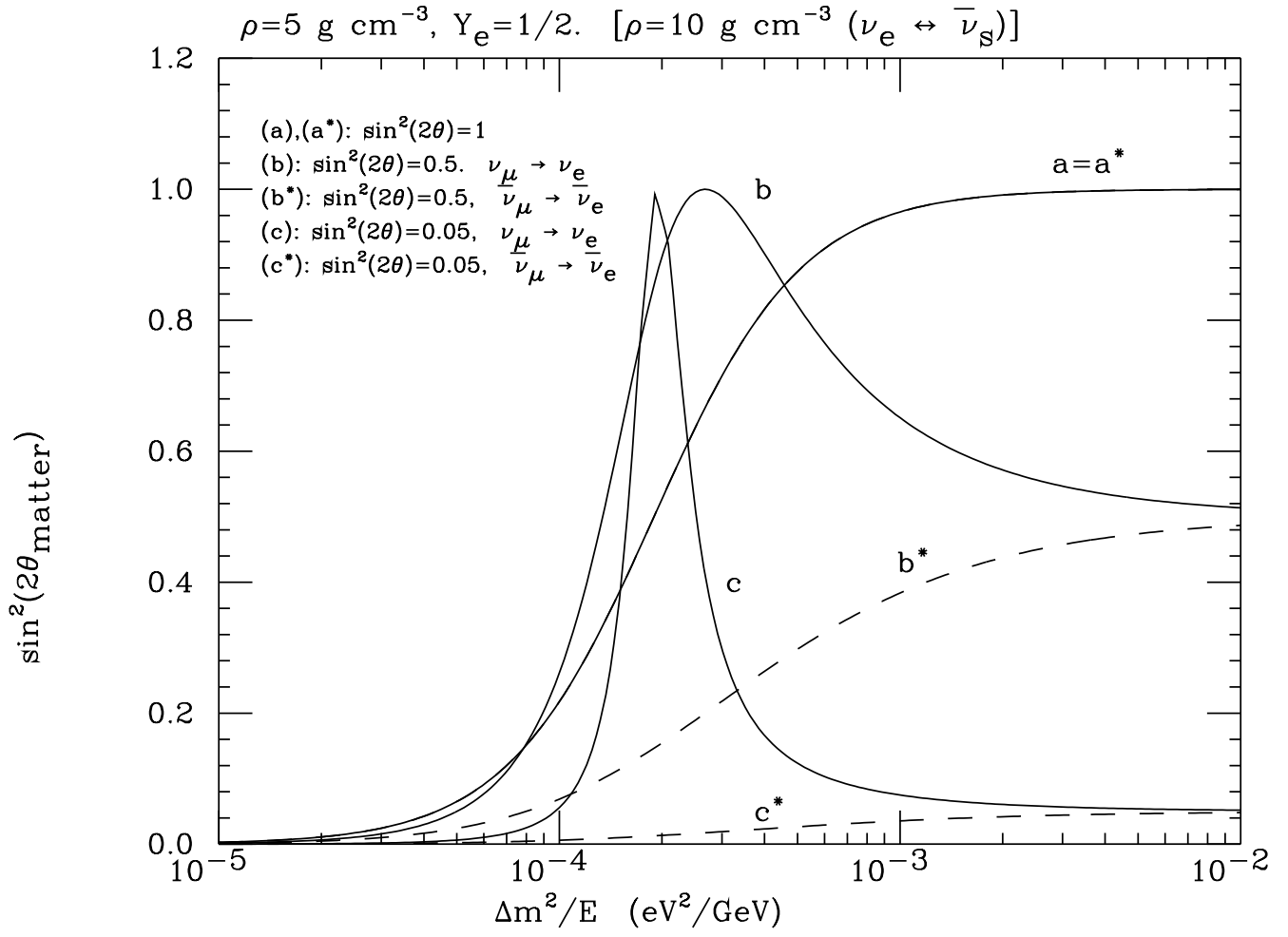


Figure 1

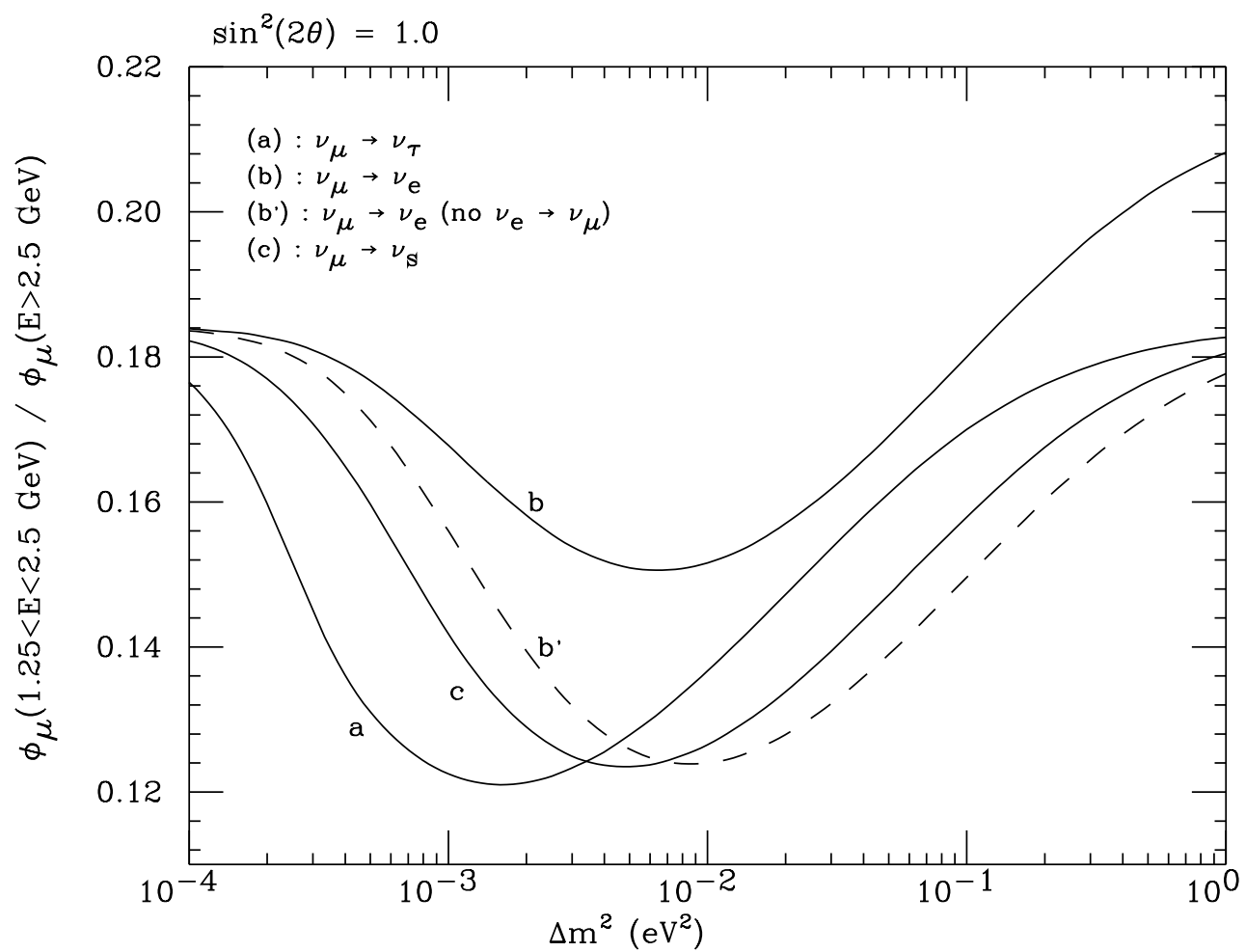


Figure 2

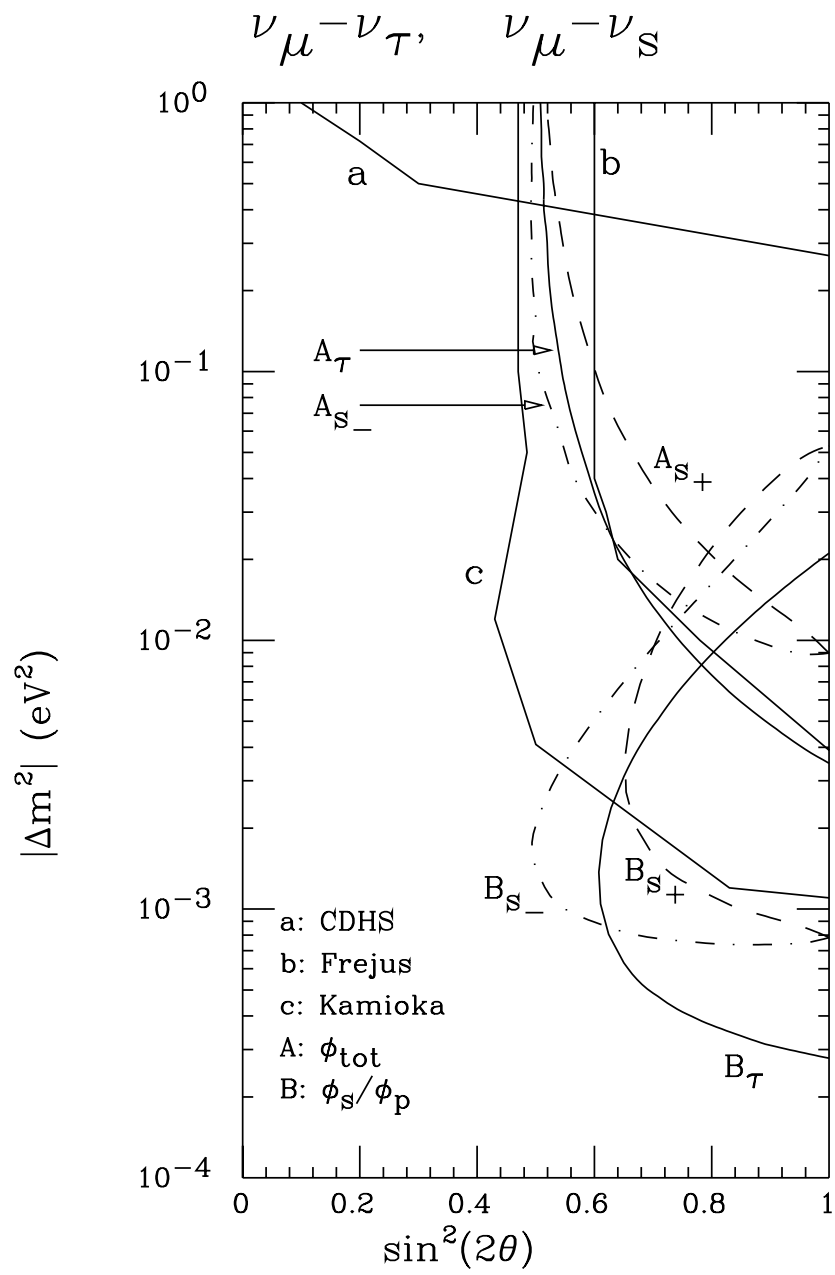


Figure 3



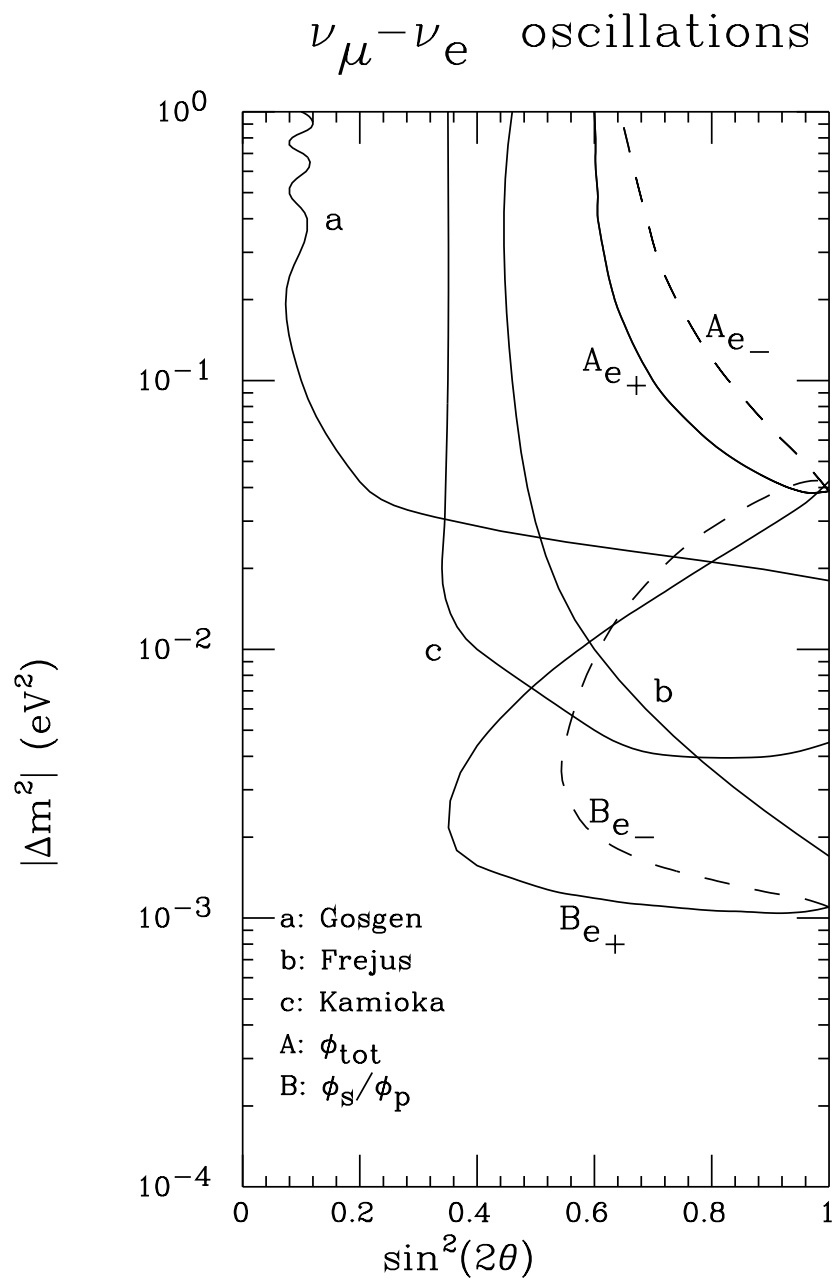


Figure 4